Available online at www.rilem.net

Materials and Structures **38** (December 2005) 857-864

Performance of hybrid rebars as longitudinal reinforcement in normal strength concrete

B. Saikia, J. Thomas, A. Ramaswamy and K. S. Nanjunda Rao
Department of Civil Engineering, Indian Institute of Science, Bangalore- 560012, INDIA

Received: 22 November 2004, accepted: 29 November 2004

ABSTRACT

Although steel is most commonly used as a reinforcing material in concrete due to its competitive cost and favorable mechanical properties, the problem of corrosion of steel rebars leads to a reduction in life span of the structure and adds to maintenance costs. Many techniques have been developed in recent past to reduce corrosion (galvanizing, epoxy coating, etc.) but none of the solutions seem to be viable as an adequate solution to the corrosion problem. Apart from the use of fiber reinforced polymer (FRP) rebars, hybrid rebars consisting of both FRP and steel are also being tried to overcome the problem of steel corrosion. This paper evaluates the performance of hybrid rebars as longitudinal reinforcement in normal strength concrete beams. Hybrid rebars used in this study essentially consist of glass fiber reinforced polymer (GFRP) strands of 2 mm diameter wound helically on a mild steel core of 6 mm diameter. GFRP stirrups have been used as shear reinforcement. An attempt has been made to evaluate the flexural and shear performance of beams having hybrid rebars in normal strength concrete with and without polypropylene fibers added to the concrete matrix.

RÉSUMÉ

Bien que l'acier soit communément utilisé comme matériau de renforcement en raison de la compétitivité de son coût et de ses propriétés mécaniques avantageuses, le problème de la corrosion de barres en acier conduit à une réduction de la durée de vie de la construction et augmente les coûts d'entretien. De nombreuses techniques ont été récemment développées afin de réduire la corrosion (galvanisation, revêtement par peinture aux résines époxydiques, etc.) mais aucune de ces solutions ne semble viable pour lutter au mieux contre le problème de la corrosion. À part l'utilisation de barres d'armature en polymères renforcés de fibres (PRF), des barres d'armature hybrides composées à la fois de PRF et d'acier sont également testées pour surmonter le problème de la corrosion de l'acier. Cet article évalue les performances de barres d'armature hybrides en tant que renforcement longitudinal dans des poutres de béton à résistance normale. Les barres hybrides utilisées dans ce travail sont principalement constituées de paquets de polymères renforcés de fibres de verre (GFRP) de 2 mm de diamètre orientés suivant une configuration hélicoïdale, autour d'une carotte d'acier doux de 6 mm de diamètre. Des étriers en polymères renforcés de fibres de verre ont été utilisés comme renforcement au cisaillement. On a essayé d'évaluer le comportement en flexion et cisaillement de poutres de béton à résistance normale comportant des barres d'armature hybrides, avec et sans addition de fibres de polypropylène à la matrice du béton.

1. INTRODUCTION

Reinforced concrete is a very common building material for the construction of facilities and structures. As a complement to concrete's limited tensile strength, steel rebar is an effective and cost-efficient reinforcement. Recently, composite materials such as glass fiber reinforced polymer (GFRP) and carbon fiber reinforced polymer (CFRP) have become an attractive alternative to steel reinforcement, as these materials are non-corrosive, possesses a high strength-to-weight ratio and are commercially available for the construction industry [1, 2]. In FRP rebar reinforced beams the use of fibers as an additive in the concrete matrix to enhance the cross-sectional ductility and to improve shear resistance has also been explored in earlier studies [3, 4]. In this study, the hybrid rebars used consisted of ten, 2mm-diameter GFRP strands, helically wound on a 6mm-diameter steel rod, with the help of an epoxy binder material ensuring that there is no gap between the GFRP strands through-out the length of the rebar (Fig. 1). In earlier studies bond between the FRP reinforcement and concrete was achieved through the use of sand coating on the surface of the rebars [5] or through a secondary surface treatment of the rebars [1, 6]. It is expected that the helical winding in hybrid bars would offer adequate bond through interlocking. The principal advantage of hybrid rebar over the FRP rebar is the ductility introduced into the cross section due

doi:10.1617/14229

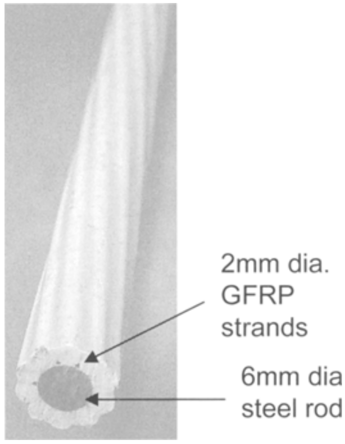

Fig. 1 - Hybrid bar (10 GFRP strands helically wound on steel core).

the presence of steel. The stress-strain curve of the hybrid rebar is similar in shape to that of steel rebar. Conventionally FRP reinforced beams are designed based either on working stress principles or as an over-reinforced beam on limit state principles. In this study, an attempt is made to study the behaviour of hybrid rebar reinforced beams, which are designed as under-reinforced section similar to design principles employed for conventional steel reinforced concrete beams.

2. EXPERIMENTAL INVESTIGATION

Firstly, tests were conducted to determine the mechanical properties of the hybrid bars and the GFRP coupon taken from the GFRP stirrup. The results from these tests have been shown in Table 1. The stress-strain curves of hybrid rebar and the GFRP stirrup are shown in Figs. 2 and 3, respectively. A pullout test was conducted to determine the bond stress of hybrid bars. The pullout specimen consisted of 152 mm by 304 mm concrete cylinder with a hybrid rebar embedded axisymmetically with an embedment length of 200 mm. Bond stress (τ_b) at failure was found to be 3.3MPa. The plot between axial stress in the rod and slip is shown in Fig. 4.

The experimental work included testing of two sets of beam specimens with moderately high strength concrete (≅48 MPa) under four point bending loads. The size of the beam was 180 x 250 x 1540 mm. Shear span and the pure moment span of the beams specimens were 420 mm and 500 mm, respectively. The first set of specimens consisted of three-flexure control beams of which one beam specimen had steel as longitudinal and transverse reinforcement and the other two were with hybrid rebar as longitudinal reinforcement and GFRP stirrups. Details of GFRP stirrup are shown in Fig. 5. The second set of specimens consisted of three, shear control beam specimens; one was with steel rebar and the remaining two were with hybrid rebar for longitudinal reinforcement. All the beam specimens were designed as under-reinforced section. Further, the design assumed that the stress in the rebars at failure would reach its ultimate stress. The nomenclature adopted to identify the beam specimens and details of all the beam specimens are indicated in Tables 2 and 3 respectively. One of the beams in each set was cast using

Table 1 - Tension test results

Specimen	Ultimate tensile strength (MPa)	Strain at ultimate load	Modulus of elasticity (MPa)
Steel bar	547.095	0.038200	228771
Hybrid bar	647.502	0.014876	101988
GFRP Stirrup (Fig. 5)	197.03	0.015420	13310

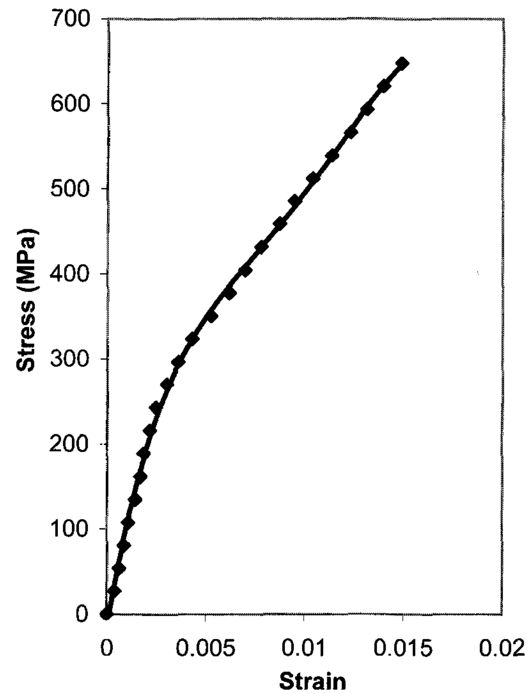

Fig. 2 - Stress-strain curve of hybrid rebar.

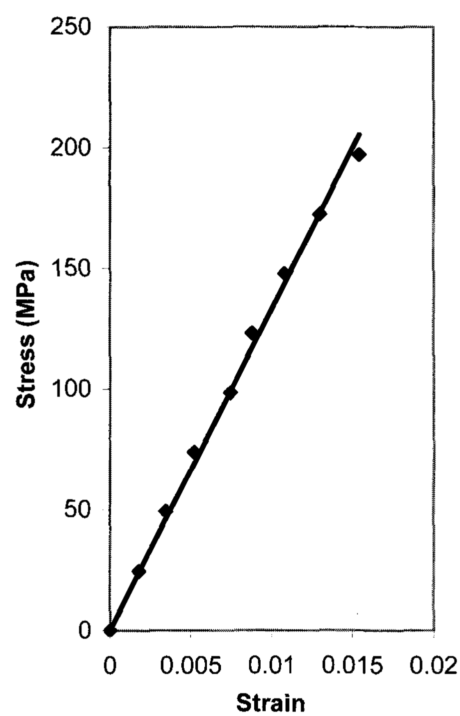

Fig. 3 - Stress-strain curve of GFRP stirrup.

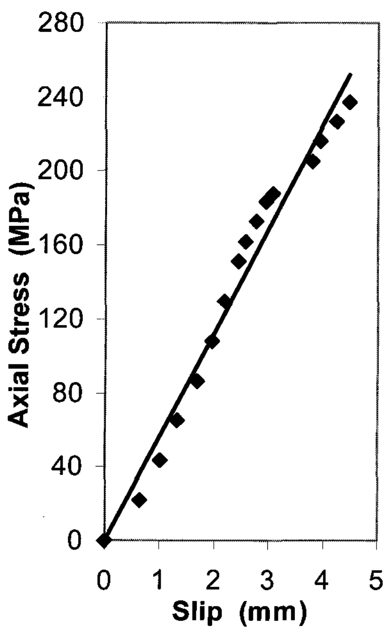

Fig. 4 - Axial stress v/s slip from pullout test of hybrid rebar.

Table 2 - Nomenclature adopted for identification of beam specimens

Type of beam	"F" for flexure control
	"S" for shear control
Type of longitudinal reinforcement	"S" for ferrous steel
	"H" for hybrid rebar
Type of transverse reinforcement	"S" for ferrous steel
	"G" for GFRP
Type of concrete	"OC" for plain concrete
	"FC" for concrete with polypropylene fibres

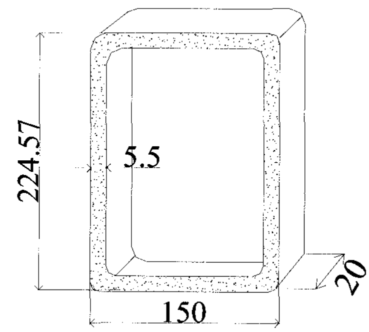

Fig. 5 - Details of GFRP stirrup (All dimensions in mm).

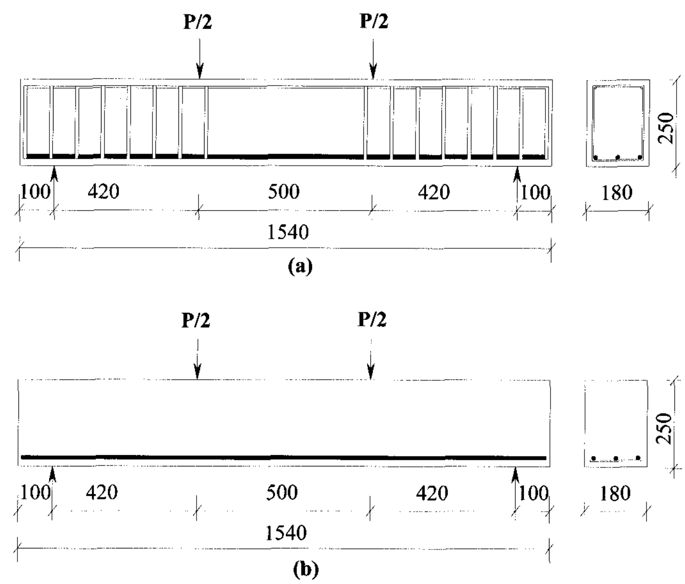

Fig. 6 - Schematic diagram of reinforcement details in (a) flexure control beam and (b) shear control beam (All dimensions in mm).

0.1% by weight of cement of polypropylene fibers introduced into the concrete matrix. Schematic details of beam reinforcement are shown in Fig. 6. All the beam specimens were tested as simply supported members subjected to four-point loading. Strain gages were fixed to the hybrid rebars and steel longitudinal bars at mid-span. Strain gages were also fixed to the surface of the concrete in the flexure zone. Linear Variable Differential Transducers (LVDT) and digital dial gages were used to measure the vertical displacement at mid-span and quarter-span of each specimen.

Table 3 - Details of beam specimens and their target design loads

Beam specimen	Type of rebar	f_{ck}^* (MPa)	Target design load (kN)	Longitudinal reinforcement	Transverse reinforcement	Additives
Flexure control beam specimens						
FSSOC	Steel	54.46	197.4	2-12mm and 2- 10mm	8mm-2legged @120mm c/c	None
FHGOC	Hybrid bars	47.94	181.3	3-10.862mm	20x5.5mm @120mmc/c$	None
FHGFC		48.38	181.3	3-10.862mm	20x5.5mm @120mmc/c$	Polypropylene Fibers
Shear control beam specimens						
SSOC	Steel	48.84	106.7	2-12mm and 2-10mm	None	None
SHOC	Hybrid bars	46.54	93.3	3-10.862mm	None	None
SHFC		47.44	93.3	3-10.862mm	None	Polypropylene Fibers

$Close loop GFRP stirrup (Fig. 5)
*150mm cube compressive strength of concrete
Note: Maximum size of coarse aggregate used in concrete is 20mm

3. TARGET DESIGN STRENGTH OF BEAMS

Hybrid rebar reinforced concrete beams have been designed assuming that perfect bond exists between rebar and surrounding concrete until the failure of the beam. The flexural capacity of the beam has been estimated based on the premise that the limiting strain in the extreme compression fiber of concrete ($\varepsilon_{c,lim}$ = 0.003) and the ultimate tensile strain in the hybrid rebar ($\varepsilon_{hyb,ult.}$= 0.015) will reach simultaneously. The strength of shear control beams has been estimated considering the shear capacity of concrete and dowel action of the longitudinal reinforcement. The target design load of all the beams tested is shown in Table 3.

4. SHEAR ANALYSIS OF CROSS-SECTIONS

The shear strength of the reinforced concrete beams determined from the tests on the shear control beams having steel or hybrid reinforcements has been compared with the shear strengths predicted using the equation proposed by Padmarajaiah and Ramaswamy [7] and those recommended in ACI 318-(2002) [8].

The equation proposed by Padmarajaiah and Ramaswamy [7] is based on separation of shear capacity contributions obtained from beam and arch mechanism. Further, the model accounts for fiber characteristics including pullout resistance and influence of fibers on split cylinder strength [9]. The ultimate shear strength equation considers the effects of fibers on the aggregate interlock and dowel action, fiber effects on the tensile prestressing and non-prestressing steel, and the effect of fibers pull-out stresses across the cracks and is expressed as:

$$v_{uf} = \varsigma\left[\bar{e}\left\{0.32\left(\frac{\sqrt{f_{ckf}}}{3} + 1.918RI\right) + 75\rho\frac{d}{a}\right\} + \hat{g}v_b\right] \tag{1}$$

where RI is the reinforcing index which is the product of volume fraction of fibers (v_f) and aspect ratio of fibers (L_f/d_f), f_{ckf} is the cube compressive strength of fiber-reinforced concrete, ρ is the longitudinal tensile reinforcement ratio, d is the effective depth of beam, a is the shear span, ς accounts for the effect of maximum aggregate size (d_a) and has been given by Bažant and Kim [10] (assumed to be valid for all sizes of aggregate) as:

$$\varsigma = \frac{1}{\sqrt{1 + \dfrac{d}{25d_a}}} \tag{2}$$

$\bar{e}$ is a nondimensional arch factor that takes into account the effect of arch action. Narayanan and Darwish [11] have suggested values for the arch factor as a function of the a/d ratio. They have recommended that $\bar{e}$ takes a value of 1 when a/d > 2.8, a value of 2.8 d/a when a/d lies between 1.0 and 2.8, and a value of 1.5 when a/d < 1. The coefficient $\hat{g}$ = 1 for a/d > 2.8 and 1.3 for a/d ≤ 2.8. v_b represents the fibre pullout contribution towards the shear strength of the beam. More details on development of Equation (1) are given in [7]. For beam specimens tested in this study, Equation (1) is modified by ignoring the prestressing and the fiber term as:

$$v_{uf} = \varsigma\left\{\bar{e}\left(0.32\frac{\sqrt{f_{ckf}}}{3} + 75\rho\frac{d}{a}\right)\right\} \tag{3}$$

For beams reinforced with steel and hybrid rebars, the predicated shear strength has also been computed based on the equation recommended in ACI 318 [8] as:

$$V_c = \left[0.16\sqrt{f_c^{'}} + 17.2\rho\frac{V_u d}{M_u}\right]bd \leq 0.29\sqrt{f_c^{'}}\,bd \tag{4}$$

Comparisons of predicted shear strength and the experimental shear strengths are shown in Table 4.

Table 4 - Comparison of predicted and experimental shear strengths in shear control beam specimen

Beam designation	Experimental shear strength (kN)	Predicted shear strength (kN)	
		Padmarajaiah & Ramaswamy [7]	ACI-318 [8]
SSOC	103.0	56.5	43.9
SHOC	53.8	50.4	42.0
SHFC	51.2	50.8	42.4

5. RESULTS AND DISCUSSION

The ultimate tensile strength of hybrid rebar is about 1.18 times that of steel rebar (550 MPa) while that of GFRP stirrup is found to be 0.36 times of steel rebar. The moduli of elasticity of hybrid rebar and GFRP stirrup is only about 0.445 times and 0.0582 times of steel rebar (200 GPa), respectively.

5.1 Assessment of flexure control beam specimens reinforced with steel and hybrid rebars

Beam FSSOC having longitudinal and transverse steel rebars was used as a control beam for comparison with beams reinforced with hybrid rebars for assessing the effectiveness of hybrid rebar in flexure. Beam FSSOC was designed as an under-reinforced, flexure critical beam. This beam was designed for an ultimate load of 197.4 kN and it failed at 226 kN. The failure pattern observed was one of diagonal crushing and splitting of concrete at reinforcement level at the supports within the shear span. The shear span/depth ratio for the beam is less than 2. Figs. 7, 8 and 9 shows the comparison of strain in extreme compression fiber, strain in reinforcement, and mid-span deflection, respectively, of the test result for beams FSSOC, FHGOC and FHGFC.

Beam FHGOC having longitudinal hybrid rebars and GFRP as stirrup was designed with a capacity of 181.3 kN.

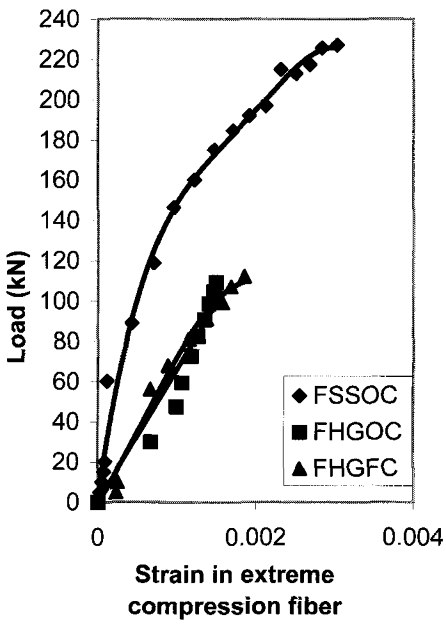

Fig. 7 - Load v/s strain in extreme compression fiber in specimen FSSOC, FHGOC and FHGFC.

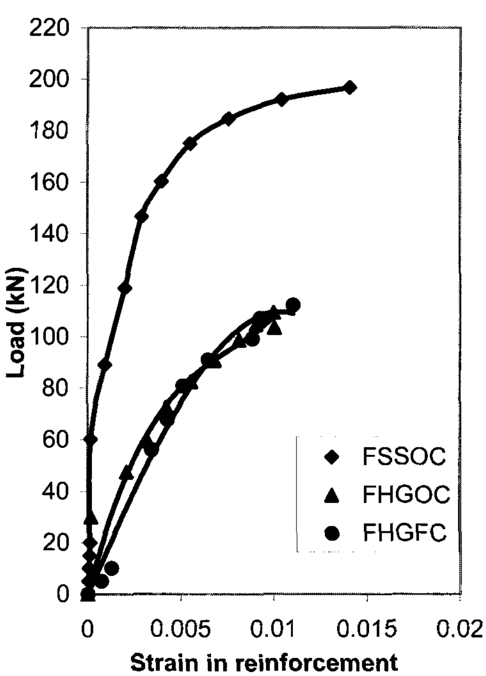

Fig. 8 - Load v/s strain in reinforcement in specimen FSSOC, FHGOC and FHGFC.

This beam has failed at a load of 109.4 kN. The mode of failure was of flexure-shear. Splitting of concrete at the reinforcement level was observed in the shear span. Ultimate failure load has occurred at about 60 percent of the designed load. Stress in hybrid rebar measured at the failure load was 500.14 MPa, which is less than the ultimate stress of hybrid rebar (647 MPa). Failure of beam at lower load is mainly due to slip between the concrete and the rebar. Due to low modulus of elasticity of hybrid rebars deflection observed is much higher at the same loading stages when compared to FSSOC (Fig. 9).

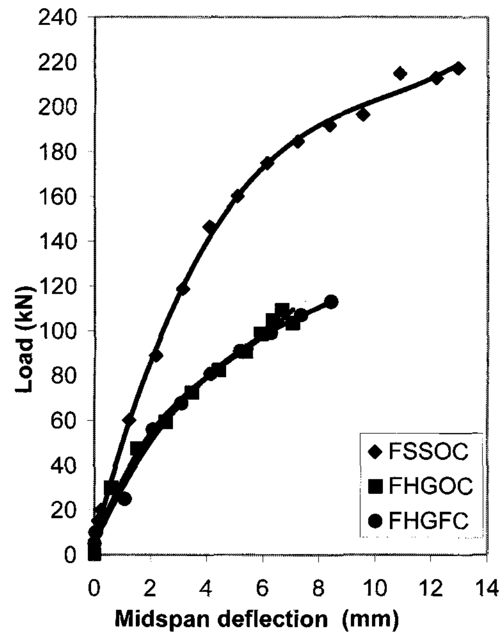

Fig. 9 - Load v/s deflection in specimen FSSOC, FHGOC and FHGFC.

Beam FHGFC was designed for load of 181.3 kN with hybrid rebars as longitudinal reinforcement, GFRP as stirrup and with polypropylene fibers in concrete in order to access the performance of hybrid rebars as longitudinal reinforcement in presence of fibers in concrete. The failure load of this beam was 112.2 kN and the beam has failed in flexure-shear mode. Splitting of concrete was observed at the reinforcement level in the shear span. This beam has failed at about 61 percent of designed load. Failure at lower load is due to slip between the concrete and rebar. It was not able to assess the performance in load carrying capacity of this beam due to the presence of fibers in concrete as the beam failed prematurely due to slip of hybrid rebar from the concrete. Nevertheless a marginal increment in the load carrying capacity was observed when compared to FHGOC. Deflection observed in this beam at the same loading stage is much higher than FSSOC but the deflection is almost the same as that of FHGOC (Fig. 9).

The design of hybrid rebar reinforced concrete beams was based on a cover to reinforcement of about 25mm, which is typical of steel reinforced concrete beams. The mode of failure observed in the tests (delamination at the level of reinforcement leading to anchorage failure) in the present investigation suggests that cover to reinforcement is inadequate. This might have led to premature failure of beams, resulting in not realizing the target ductility.

5.2 Assessment of shear control beam specimens reinforced with steel and hybrid rebars

Beam SSOC was reinforced with longitudinal steel rebars and used as a control beam to make comparison with beams reinforced with hybrid rebars in order to assess the performance of hybrid rebars in shear. This beam was designed for an ultimate load of 106.7 kN and has failed at a load of 206.0 kN. This beam failed in flexure-shear mode. In

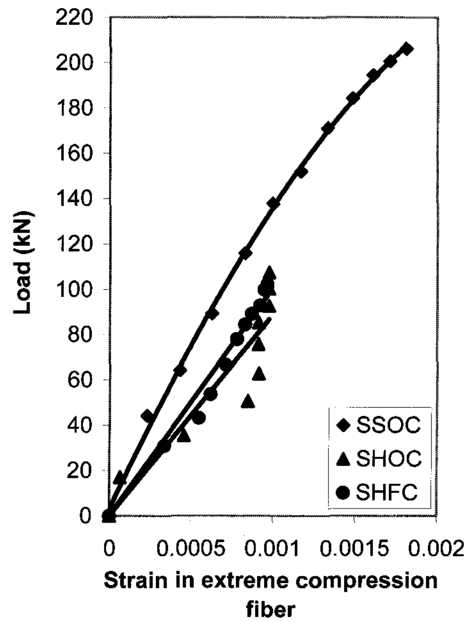

Fig. 10 - Load v/s strain in extreme compression fiber in specimen SSOC, SHOC and SHFC.

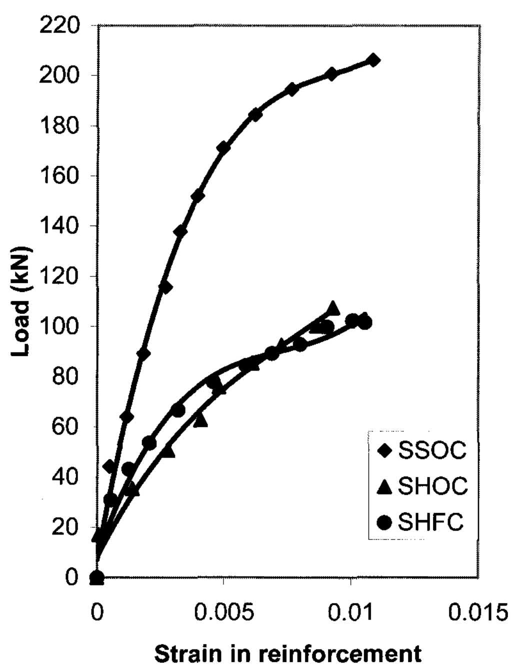

Fig. 11 - Load v/s strain in reinforcement in specimen SSOC, SHOC and SHFC.

addition, splitting of concrete at reinforcement level was observed. Figs. 10, 11 and 12 show the comparison of load v/s strain in compression, load v/s strain in reinforcement and load v/s mid-span deflection for beams SSOC, SHOC and SHFC.

Beam SHOC was reinforced with hybrid rebars and the ultimate designed load for this beam was 93.3 kN. Failure load of this beam was 107.6 kN and the mode of failure was flexure-shear. Due to low modulus of elasticity of rebars, deflection in beam SHOC was much higher than SSOC at the same loading stage (Fig. 12).

Beam SHFC was reinforced with hybrid rebars with polypropylene fibers in concrete in order to assess the performance of hybrid rebars in shear in presence of fibers. This beam was designed for a load of 93.3 kN. Ultimate load observed at failure was 102.4 kN. The failure mode observed in this beam was flexure shear. Performance of fibers in concrete could not be assessed as the slip between concrete and rebars controlled the failure. Though the deflection was much higher compared to SSOC but the deflection was comparable to beam SHOC at the same load (Fig. 12).

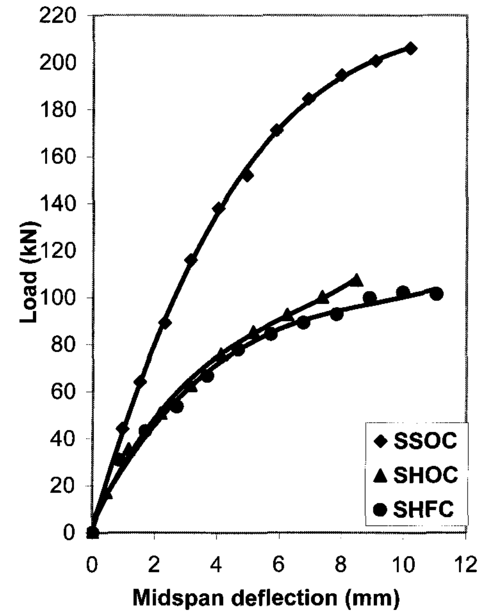

Fig. 12 - Load vs. deflection in specimen SSOC, SHOC, and SHFC.

From Table 4 it can be seen that the computed shear strength of beam specimens SHOC and SHFC based on [7] and [8] using the values of $\bar{e}$ recommended by Narayanan and Darwish [11] are in good agreement with the experimental results. However, for beam SSOC the computed shear strength value is far less compared to the experimental value.

6. FLEXURAL ANALYSIS OF BEAMS ACCOUNTING FOR SLIP OF HYBRID REBAR

Tests on beams reinforced with hybrid rebar have revealed that the failure of the beams was due to loss of bond between rebars and the concrete. Hence the beams did not achieve the target design strengths. An attempt has been made here to develop an analytical model which accounts for loss of bond between rebar and concrete and thus to predict the failure load of beams. The model is based on the bond strength (τ_b) and slip strain (ε_{slip}) obtained from the concentric pullout test results. For calculating the development length (L_d) of the rebar in the beam, it is assumed that a critical inclined crack will be formed from the load point and will meet the base of the beam at a distance equal to the effective depth of the beam from the loading point as shown in Fig. 13. From Fig. 13, the development length for rebars is equal to (shear span + bearing

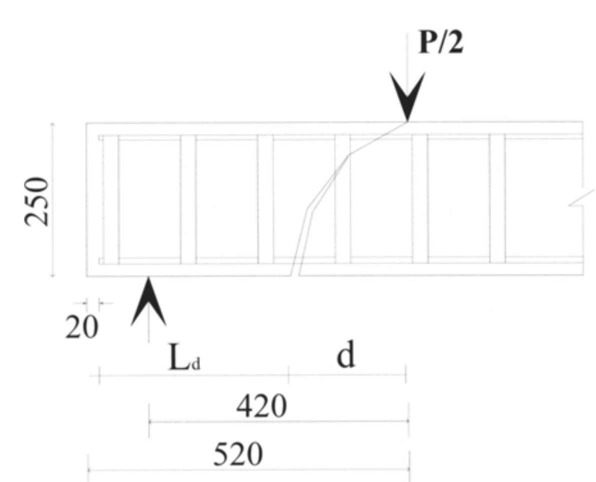

Fig. 13 - Development length in hybrid rebar reinforced beam specimen.

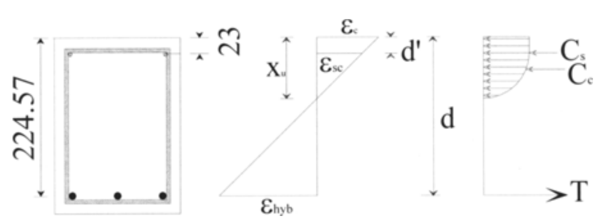

Fig. 14 - Stress-strain block diagrams.

length – cover – effective depth of the beam). From Fig. 14 the strain at the top fiber of concrete is given by:

$$\varepsilon_c = \frac{\varepsilon_{slip}}{(d - x_u)} x_u \,. \qquad (5)$$

Compressive force in concrete 'C_c' is:

$$C_c = \frac{2}{3} b f_{ck} \left[-\left(\frac{\varepsilon_c}{0.002} \right)^2 + 2 \frac{\varepsilon_c}{0.002} \right] x_u \qquad (6)$$

When $\varepsilon_c \leq 0.002$

$$C_c = \frac{2}{3} b f_{ck} \frac{0.002}{\varepsilon_c} x_u + b \left(x_u - \frac{0.002}{\varepsilon_c} x_u \right) f_k \qquad (7)$$

When $\varepsilon_c > 0.002$

From Fig. 14 the strain in the hanger bar is:

$$\varepsilon_{sc} = \frac{\varepsilon_c}{x_u} (x_u - d') \,. \qquad (8)$$

Stress in the hanger bar 'f_{sc}', is obtained from the stress strain relationship of the hanger bar material. It is assumed that the strain in the hanger bars is the same as the concrete strain at the level of hanger bars. Compressive force in hanger bar is:

$$C_s = f_{sc} A_{sc} \qquad (9)$$

Total compressive force, $C = C_c + C_s$ (10)

Total tensile force, $T = (\tau_b \, \pi \, \Phi L_d)$(number of rebars) (11)

where ϕ is the diameter of the rebar. The average bond strength (τ_b) and the strain in the rebar at slip (ε_{slip}) obtained from pullout test were found to be 3.3MPa and 0.005274 respectively. For equilibrium of forces in the cross-section, C + T = 0. By trial and error process, neutral axis depth 'x_u' is determined. Upon determining 'x_u', failure moment and load are computed. The predicted failure load for beams FHGOC and FHGFC is found to be 94.9kN and is presented in Table 5. It can be seen that predicted failure load is in satisfactory agreement with the experimental failure load.

Table 5 - Comparison of failure load in flexure control beam specimen

Beam designation	Experimental load (kN)	Predicted by analytical model accounting for slip of hybrid rebar (kN)	Mode of failure
FSSOC	226.0	----	Flexure – shear
FHGOC	109.4	94.9	Flexure-shear
FHGFC	112.2	94.9	Flexure - shear

7. CONCLUSIONS

The following conclusions emerge from the present study:

- Tensile strength of hybrid rebar used in the present study is slightly higher than steel. The modulus of elasticity of the hybrid rebars is about 50 percent of the value for steel rebars.
- For the same load greater deflections were observed for hybrid rebar reinforced beams specimens compared to conventional steel reinforced beams.
- Failure of hybrid rebar reinforced beams was primarily due to delamination at the level of reinforcement, leading to anchorage failure, resulting in loss of bond between rebar and concrete. The above mode of failure must have led to their premature failure.
- There exists a need to improve the bond between concrete and hybrid rebar.
- The concrete cover of 25mm, kept constant in all beams, appears to be inadequate for hybrid rebar reinforced concrete beams.
- The analytical model accounting for slip of the hybrid rebar developed for predicting the failure load is in satisfactory agreement with experimentally observed failure load of beams.
- Failure modes observed in shear control beams reinforced with hybrid rebars were similar to that of steel reinforced beams. However the shear strength of

the beams reinforced with the hybrid rebars is found to be significantly lower than the beam with steel bar as longitudinal reinforcement.

ACKNOWLEDGEMENTS

The authors would like to acknowledge the financial support received from the Department of Science and Technology, Government of India, New Delhi for carrying out this project (Grant No. II.3 (3)/99-ET/9-11-2000).

REFERENCES

[1] Sonobe, Y., Fukuyama, H., Okamoto, T., Kani, N., Kimura, K., Kobayashi, K., Masuda, Y., Matsuzaki, Y., Mochizuki, S., Nagasaka, T., Shimizu, A., Tanano, H., Tanigaki, M., and Teshigawara, M., 'Design guidelines of FRP reinforced concrete building structures', *Journal of Composites for Construction, ASCE* **1** (4) (1997) 90-114.

[2] Yost, J.R., Gross, S.P. and Dinehart, D.W., 'Shear strength of normal strength concrete beams reinforced with deformed GFRP bars', *Journal of Composites for Construction, ASCE* **5** (4) (2001) 268-275.

[3] Kuntia, M., Stojadinovic, B. and Goel, S.C., 'Shear strength of normal and high-strength fiber reinforced concrete beams without stirrups', *ACI Structural Journal* **96** (2) (1999) 282-289.

[4] Banthia, N. and Mani, M., 'Behaviour of non-prestressed GFRP reinforcement and a fibrous concrete matrix', Proc. of R.N. Swamy Symposium, Real World Concrete, Proc. 5th CANMET/ACI International Conference on Flyash, Slag and Natural Pozzolans in Concrete, Milwaukee, 1995, 71-94.

[5] Kumar, L.K., Ramaswamy, A. and Rao, K.S.N., 'Behavior of GFRP reinforced SFRC beams in flexure and shear", Advances in Civil Engineering, edited by Bandyopadhyay, J.N., and Nagesh Kumar, IIT Kharagpur, Allied Publishers, New Delhi, 2002, 1151-1157.

[6] Saikia, B.P., Kumar, P., Thomas, J., Rao, K.S.N. and Ramaswamy, A., 'A study on flexural performance of beams reinforced with GFRP bars', Proceedings of the ICFRC-International Conference on Fiber Composites, High Performance Concretes and Smart Materials & Workshop on High Volume Fly Ash Concrete, Chennai, 2004, 465-474.

[7] Padmarajaiah, S.K., and Ramaswamy, A., 'Behavior of fiber reinforced prestressed and reinforced high-strength concrete beams subjected to shear', *ACI Structural Journal* **98** (5) (2001) 752-761.

[8] ACI-318, 'Code of Practice for Plain and Reinforced Concrete Structures', Published by American Concrete Institute, Detroit, Michigan (2002).

[9] Padmarajaiah, S.K. and Ramaswamy, A., 'Comparative study on flexural response of full and partial depth fiber-reinforced high-strength Concrete', *Journal of Materials in Civil Engineering (ASCE)* **14** (2) (2002) 130-136.

[10] Bažant, Z.P. and Kim, Jin-Keun, 'Size effect in shear failure of longitudinally reinforced beams', *ACI Journal Proceedings* **81** (5), (1984) 456-468.

[11] Narayanan, R. and Darwish, I.Y.S., "Use of steel fibers as shear reinforcement", *ACI Structural Journal* **84** (3) (1987) 216-227.